Fusion of Regularization Terms For Image Restoration

Max Mignotte

***Abstract*— In this paper, we propose an efficient regularized restoration model associating a spatial and a frequential regularizer in order to better model the intrinsic properties of the original image to be recovered and to obtain a better restoration result. An adaptive and rescaling scheme is also proposed to balance the influence of these two different regularization constraints, preventing an overwhelming importance for one of them from prevailing over the other, enabling them to be efficiently fused during the iterative deconvolution process. This hybrid regularization approach, mixing these two constraints and more precisely, favoring a solution image that is both efficiently denoised (due to the denoising ability of a thresholding procedure in the DCT domain) and edge-preserved (due to the GGMRF constraint), yields significant improvements in terms of image quality and higher ISNR results compared to a single GGMRF or DCT prior model, and leads to competitive restoration results in benchmark tests, for various levels of blur, BSNR and noise degradations.**

***Index Terms*— Regularized iterative restoration/deconvolution methods, fusion of regularization terms, mix of multiple constraints, generalized Gaussian Markov random field (GGMRF) prior model, discrete cosine transform, spatial and frequential regularizers.**

I. Introduction

In regularized restoration approaches, the regularization term allows us both to stabilize (from the computational viewpoint) the solution to the ill-conditioning restoration inverse problem and to incorporate knowledge or beliefs concerning the types of restorations *a priori* defined as acceptable solutions. That is why the design of efficient image prior models or a priori regularization terms, and especially their ability to (locally and globally) summarize the intrinsic properties of the original image to be recovered, are crucial in the final image quality and signal-to-noise improvement (ISNR) restoration result.

Over the last two decades, there have been considerable efforts to find a regularization term capable of both efficiently denoising the image and preserving its local discontinuities, i.e., its edges. To this end, several edge-preserving regularization strategies were proposed (with some notable improvements in the restoration results) in the spatial [1]–[8] domain *via* a non-stationary, compound Markov model with possibly robust estimators or variational approaches, or in the frequency domain, by also promoting a restored image having a high sparsity of its spectral coefficients, *via* thresholding operations in the wavelet domains [5], [6], [9]–[14].

[1]Max Mignotte is with the Département d'Informatique et de Recherche Opérationnelle (DIRO), Université de Montréal, C.P. 6128, Succ. Centre-ville, H3C 3J7, Montréal (Québec). E-mail: mignotte@iro.umontreal.ca

In order to circumvent the difficulty of finding a single regularization term that summarizes all the contradictory and intrinsic properties of an undegraded image (such as homogeneity of the desired solution and local edge model), another strategy is to find a framework that combines several (contradictory but complementary) terms of regularization or prior models. To this end, some attention has been given to associating/combining two different (but complementary) regularization terms and/or equivalently to proposing a regularization strategy that enforces simultaneously multiple (and different) constraints in order to improve the final restoration result. Indeed, some of the well-known regularization priors are conceptually very different; either local and expressed in the spatial domain or more or less global and expressed in the (DCT, wavelet or Fourier) frequency domain. A hybrid regularization approach, mixing two or several of these, could efficiently better model the complex properties of the class of images *a priori* defined as acceptable solutions for a better final restoration result.

In this attempt to combine both a regularization approach exploiting a frequency representation (e.g., wavelet) and a spatial penalty term (such as the one implicitly used in variational approaches [8]), some hybrid regularization strategies have already been proposed. In [15], the author proposes to seek a restored image that has minimum total variation (i.e., whose integral of the gradient Euclidean norm is minimal) under the constraint that the residual image r (i.e., $\hat{x} * h - y$ where h, x and y are respectively the blur, the estimated image, and the observed image) belong to a wavelet basis Ψ with $|<r, \Psi>| < \tau$ (and $\tau > 0$). These latter local constraints aim at controlling that the residual image is in fact a white noise that does not contain any structure or detail from the undegraded image. It is worth mentioning that in this combination of two regularizers, the total variation (L_1 optimization) regularizer is used to damp ringing artifacts near edges caused by the oscillations of the wavelet atoms, and on the other hand, the wavelet decomposition and thresholding alleviates the staircase effect of L_1 optimization. A similar model but exploiting a curvelet decomposition for a pure denoising application is also proposed in [16]. In a somewhat similar spirit, Durand and Froment [17] propose to combine these two regularization approaches and thus to address the problem of ringing artifacts in wavelet denoising by replacing the thresholded wavelet coefficients by coefficients that minimize the total variation. Their method is also closely related to approaches by Chan [18] who post-processed images obtained from wavelet shrinkage by a total variation-like denoising technique. Let us also note that these previously mentioned techniques are

specifically *designed* to combine the total variation approach and the wavelet thresholding technique and cannot be generalized in order to combine several other regularizers or penalty terms.

Another strategy consists in the estimation/combination of an image segmentation result with a DCT-based restoration procedure [2]. In this context, Foi *et al.* [2] propose to apply a DCT filtering computed on several polygonal supports whose shape are defined by a preliminary segmentation technique estimated on a (deblurred) image. The segmentation technique, which was preliminarily used in this restoration procedure, implicitly exploits an image prior model expressing that any real-world images can be approximated by a union of a number of nonoverlapping and distinct regions (of uniform grey level value). The restoration procedure proposed in [2] thus indirectly combines this segmentation-based prior model with a regularization prior expressed in the DCT domain. However, let us also note that this strategy is also specifically *designed* to combine a segmentation result and a DCT filtering technique and cannot be generalized in order to combine several other regularizers or penalty terms.

A simple strategy to combine two different penalty functions consists of introducing these two regularizing terms directly in the cost function to be optimized with, for example, two adaptive weights, generally proportional to the residual image r [19]. Another strategy consists of the combination of the two penalty terms *via* an edge indicator function (controlled by the observed image) switching between them, such as that defined (somewhat similarly) in [20], [21] in which the total variation penalty term and a fourth-order filter are conjointly used in order to preserve edges while avoiding the staircase effect in smooth regions. In a more general way, to fuse several constraints or equivalently several prior knowledges for the image to be recovered, a Bayesian strategy has been recently proposed in [22]–[24] which uses a statistical prior in product form. Such product type priors combine multiple image prior models by assuming that the local discontinuities of the image (i.e., its edges) given by different local edge models (i.e., different high-pass filters) are Student-t distributed. In order to bypass the difficulty of evaluating the normalization constant of this product type prior, the authors in [22]–[24] propose to use a constrained variational approximation methodology to infer the restored image.

The approach proposed in this paper is different and uses another fusion strategy. More precisely, our model simply exploits an additional constraint (called in the following "rescaling operation") whose goal is to iteratively balance the influence of two (but possibly several) different penalty functions, expressed by each image prior model, during a simple iterative Landweber deconvolution process. In addition, compared to [22], [23], our approach tends to enforce two different regularization strategies, respectively expressed in the spatial and frequential domain, by promoting a restored solution both efficiently denoised due to a DCT denoising procedure [25]–[27] and edge-preserved due to a GGMRF prior model [28].

More generally, the concept of combining several classifiers, models or constraints for the improvement of the performance, or (in our application) to better model the complex properties of the class of images to be recovered by a restoration algorithm, is known, in the machine learning field, as a committee machine or mixture of experts [29], [30]. In this recent field of research, two major categories of committee machines are generally found in the literature. Our fusion approach is in the category of the committee machine model that utilizes an ensemble of models or experts with a dynamic structure type. In this class of committee machines, the set of constraints is combined by means of a mechanism that involves the input data (contrary to the static structure type-based mixture of experts).

The remainder of this paper is organized as follows: Section II describes the proposed model with respectively the edge sparseness and the sparse representation constraints and last the proposed fusion approach of these two constraints in an iterative deconvolution Landweber process. Last, section III presents a set of experimental results and comparisons with existing restoration techniques.

II. Proposed Approach

A. Edge Preserving Constraint in the Spatial Domain

The first regularization term used in our restoration model is formulated in the (image) spatial domain and promotes a (regularized) restored image $\hat{x}$ with spatial smoothness and edge-preserving properties. To this end, we have considered the GGMRF prior model proposed by Bouman and Sauer in tomographic reconstruction [28], [31]. This prior has a density function of the form $P_X(x) \propto \exp\{-\gamma\,\Omega(x)\}$ with the following regularization term

$$\Omega(x) = \sum_{<s,t>} \beta_{st} |x_s - x_t|^q \tag{1}$$

where $1 \leq q \leq 2$ is a parameter controlling the smoothness of the image to be recovered and/or the sharpness of the edges to be formed in the restored image. $\beta_{st} = (2\sqrt{2}+4)^{-1}$ or $(4+4\sqrt{2})^{-1})$ depends on whether the pair of neighboring sites (relative to the second order neighborhood system), or binary clique $<s,t>$ is horizontal/vertical or right diagonal/left diagonal. This prior model has the advantage of including a Gaussian MRF prior for $q = 2$ and a more interesting edge-preserving absolute-value potential function with $q = 1$ somewhat similar to the L_1 regularizer proposed by Rudin *et al.* in [8]. In the regularization framework and under this first constraint a restored image can be seen as a solution to the following penalized likelihood cost function to be optimized

$$\hat{x} = \arg\min_x \Big\{ \|y - h * x\|^2 + \gamma\,\Omega(x) \Big\} \tag{2}$$

where y and x represent respectively, the observed blurred and noisy image (degraded by an additive and white Gaussian noise with variance σ^2) and the undistorted true image. h is the Point Spread Function (PSF) of the imaging system[2] and $*$ is the linear convolution operator. For the convolution procedure, we herein assume that the image is toroidal, i.e., periodically repeated. The first term of this cost function expresses the

fidelity to the available data y and the second encodes the spatial smoothness and the local edge-sparsity constraint (i.e., the expected properties) of the true undegraded image. γ is the regularization parameter controlling the contribution of the two terms. A maximum penalized likelihood estimate of the undegraded image $\hat{x}$, under this GGMRF constraint, can be found by a classical gradient descent method. To this end, the derivative of $\Omega(x)$ at site s, has the following analytical expression $\Omega'(x_s) = q \sum_{<s,t>} \beta_{st} |x_s - x_t|^{q-1} \text{sgn}(x_s - x_t)$ and leads to the following iterative steepest descent procedure, which moves the penalized likelihood estimates in the negative gradient direction

$$\hat{x}^{[n+1]} = \underbrace{\hat{x}^{[n]} + \alpha^{[n]}\, h^{\#} * (y - h * \hat{x}^{[n]})}_{\hat{x}_{\text{ML}}^{[n+1]}} - \gamma^{[n]}\, \Omega'(\hat{x}^{[n]}) \quad (3)$$

where $h^{\#}(i,j) = h(-i,-j)$ (the coordinates (i,j) represent the discrete pixel locations and for h symmetric, we have $h^{\#} = h$). After derivation of Eq. (2), $\alpha^{[n]}$ is a constant equal to 1 for all n. Nevertheless we can easily speed up this iterative search procedure by adaptively changing $\alpha^{[n]}$ at each iteration according to the following equations [32]

$$\alpha^{[n]} = \frac{\|q^{[n]}\|^2}{\|h * q^{[n]}\|^2} \quad \text{with} \quad q^{[n]} = h^{\#} * (y - h * \hat{x}^{[n]}) \quad (4)$$

where, in this notation, pixels are organized in $q^{[n]}$ and in $h * q^{[n]}$ in lexicographic order as one large column-vector. For $\gamma^{[n]} = 0$, the iterative procedure defined in Eq. (3) is the (accelerated) well-known Landweber algorithm [33].

B. Denoising Constraint in the Frequential Domain

The second constraint used in our restoration model is formulated in the Discrete Cosine Transform (DCT) domain by promoting a restored image efficiently denoised. To this end, a convenient way to impose this constraint consist of applying to each of these coefficients (of each individual block of size 8×8 pixels of $\hat{x}^{[n]}$), a simple thresholding operation. An example of such constraint in the frequency domain is the so-called soft-thresholding operation classically used in the wavelet based denoising approach [14], [34], [35]) of each DCT coefficient, according to the following rule

$$\lambda_T^{\text{soft}} = \text{sgn}\,(w)(|w| - T)_+ \quad (5)$$

where $(.)_+$ is defined as $(x)_+ = \max\{x, 0\}$ and sgn(.) is the sign function (sgn$(x) = 1$, if $x \leq 0$, and sgn$(x) = -1$, otherwise). Another example is the hard version of this soft-thresholding operation, leading to the following hard - thresholding rule

$$\lambda_T^{\text{hard}} = \begin{cases} 0 & \text{if} \quad |w| \leq T \\ w & \text{otherwise} \end{cases}$$

in which T is a threshold level that acts as a regularization parameter and we recall that w is one of the coefficients obtained by the DCT transform of the block (of size 8×8 pixels) extracted from the current image estimate. These two thresholding rules enables the *a priori* sparse representation (in the DCT domain) of the solution image to be recovered, or equivalently favors a generalized Gaussian law for the distribution of these DCT coefficients [35].

In order to reduce blocky artifacts across the 8×8 block boundaries, a standard approach (already used in the wavelet denoising community) is to make this transform translation-invariant, i.e., to use the DCT of all (circularly) translated versions of the image herein assumed to be toroidal [36], [37]. This thus implies (for a set of 8×8 blocks extracted from the image) computing a set of 8 horizontal shifts and 8 vertical shifts ($= 64$) translated images which will then be DCT-denoised with the soft or hard thresholding rule and then averaged in a final step (see Algorithm 1).

It is worth mentioning that a possible restoration procedure using this single DCT denoising constraint would consist of alternating an ML estimate (see Eq. (3) with $\gamma = 0$, i.e., essentially a deblurring procedure) followed by a thresholding operation in the DCT domain (i.e., mainly a denoising procedure) until a convergence criterion is met. This procedure (called DCT-gradient in Tables 4 and 5 and also defined in Section III-A.2) will be compared (in Section III) with a restoration procedure combining this DCT constraint along with the GGRMF penalty term.

C. Fusion of Regularization Terms

The goal of this work is to propose a restoration procedure which promotes an acceptable restored image combining these two previously mentioned regularization constraints while ensuring the likelihood fidelity, i.e., by finding an estimate $\hat{x}$ ensuring an acceptable minimum for the likelihood energy $\|y - h * x\|^2$ under these two constraints. Equivalently, we would like to restrict the types of restorations (*a priori*) defined as acceptable solutions as those combining these two complementary spatio-frequential regularizing constraints.

The problem is not trivial since, the simple solution which would consists of alternating the two regularization strategies, i.e., an iteration of the gradient descent of the penalized likelihood function (Eq. (3)) followed by a DCT denoising step (Algorithm 1), leads to restoration results equal to those obtained in the case of either the exclusive use of the GGMRF regularization term or the DCT-based constraint, according to the value given to the two regularization parameters (i.e., γ for the GGMRF regularization term and T for the DCT constraint).

A rescaling problem, inherent to the fusion of these two regularization terms exists and must be treated. To this end, we have to balance the influence of these two different regularization strategies (in the sense of a criterion or another constraint), during the iterative search process of the solution image. This rescaling will avoid generating an overwhelming importance for one of the two regularization constraints over the second (thus making the fusion of the two regularization terms inefficient). This rescaling problem is somewhat identical to the one occurring in pattern classification when different features with different units are blended together. In

[2]We assume throughout this paper that the degradation model (PSF and variance of the white Gaussian noise) is known. It might be given analytically or given numerically based on previous estimations or calibration experiments.

this case, the rescaling step prevents the similarity measure (used to evaluate the distance between feature vectors) from (wrongly) giving an overwhelming importance to a feature having a larger unit range. In this work, in order to avoid generating an overwhelming importance for one of these two penalty terms over the second (and thus making the fusion of these two regularization strategies inefficient), we adaptively balance the two regularizers by adding, to the iterative search process of the restored image, the following adaptive empirical constraint:

CONSTRAINT A1:
"*The residual image added to the likelihood image, to each iteration of the iterative search process, by the GGMRF-based constraint and the DCT-based constraints should be equal in a norm sense.*"

In our application, the likelihood image ($\hat{x}_{\text{ML}}^{[n]}$) is the solution image obtained at iteration n, without the n'th constraint, i.e., the image obtained by Eq. (3) with $\gamma^{[n]} = 0$ or the so-called Landweber estimate. The residual image designates the additive correction image added (at each iteration) to the likelihood image by the presence of each constraint. In the case of the GGMRF constraint, the regularization adds, at iteration n, to the image likelihood the corrective term $\|\gamma^{[n]}\,\Omega'(\hat{x}^{[n]})\|$ (see Eq. (3) and Algorithm 2). In the case of the DCT-based denoising constraint (without the GGMRF-constraint), this residual image is simply (at each iteration n) the difference image between the DCT-denoised likelihood image minus the likelihood image, i.e., $\|\Upsilon_T(\hat{x}_{\text{ML}}^{[n+1]}) - \hat{x}_{\text{ML}}^{[n+1]}\|$. In this expression, $\Upsilon_T(.)$ designates the [DCT-THRESHOLDING-INVERSE DCT] operator with the thresholding operation according to the rule given by Equations (6) or (5) with the regularization parameter value T_{Hard}.

To summarize, our iterative procedure (see Algorithm 2) thus alternates between an ML estimation of the image to be restored (i.e., a classical Landweber iteration) plus the GGMRF penalty term and an ML estimation plus the hard-thresholding constraint in the DCT domain (see Algorithm 2). The threshold level T_{Hard} (or the regularization parameter in the DCT domain) is set according to the noise variance σ (herein assumed to be known) and the regularization parameter γ of the spatial GGMRF penalty term is adaptively estimated at each iteration of the restoration procedure, in order to respect equality constraint A1 (this estimation procedure will be made explicit in Section II-D). The following section used this additional constraint A1 in order to adaptively estimate $\gamma^{[n]}$ as a function of T during the iterative search restoration procedure.

D. Parameter Selection

In our restoration model, T is preliminary and empirically set according to the noise standard variation σ of the considered degradation model by the following procedure

$$T_{\text{Hard}} = \begin{cases} 1.6\,\sigma & \text{if} \quad \sigma^2 < 10 \\ 2.2\,\sigma & \text{if} \quad \sigma^2 \geq 10 \end{cases} \tag{6}$$

Algorithm 1
DCT-Based Denoising Step ($\Upsilon_{\text{T}}(x^{[n]})$)

$x^{[n]}$	Input image to be denoised at iteration n
$\hat{x}^{[n]}$	Denoised estimated image at iteration n
T	Threshold

for *All (*8 *horiz. and* 8 *vert.) shifts of* $x^{[n]}$ **do**

  for *All* $[8 \times 8]$ *blocks extracted from* $x^{[n]}$ **do**

    1. DCT Transform

    2. Threshold the obtained DCT coefficients w with the hard thresholding rule

$$\lambda_T^{\text{hard}} = \begin{cases} 0 & \text{if} \quad |w| \leq T \\ w & \text{otherwise} \end{cases}$$

    or the soft thresholding rule

$$\lambda_T^{\text{soft}} = \text{sgn}\,(w)(|w| - T)_+$$

    3. Inverse DCT of these thresholded coefficients

  ▷ Unshift the filtered image and store it

$\hat{x}^{[n]} \leftarrow$ Averaging of these 64 denoised images

or, for the soft-thresholding rule, by

$$T_{\text{Soft}} = \begin{cases} 0.2\,\sigma & \text{if} \quad \sigma^2 < 10 \\ 0.6\,\sigma & \text{if} \quad \sigma^2 \geq 10 \end{cases} \tag{7}$$

$\gamma^{[0]}$ is then estimated at the first iteration of our restoration algorithm and adaptively change in order to adaptively balance (for each iteration of our iterative algorithm) the residual image added to the likelihood image between the two sparseness constraints. Given T, $\gamma^{[n]}$ is thus estimated by

$$\gamma^{[n]} = \arg\min_{\gamma^{[n]}} \left\{ \left| \underbrace{\left\| \Upsilon_T(\hat{x}_{\text{ML}}^{[n+1]}) - \hat{x}_{\text{ML}}^{[n+1]} \right\|_1}_{\mathcal{B}_{\text{DCT}}} - \underbrace{\left\| \gamma^{[n]}\,\Omega'(\hat{x}^{[n]}) \right\|_1}_{\mathcal{B}_{\text{GGMRF}}} \right| \right\} \tag{8}$$

where $\|.\|_1$ is the $\mathcal{L}1$-norm and $\mathcal{B}_{\text{DCT}}$ and $\mathcal{B}_{\text{GGMRF}}$ represent respectively the residual image added to the likelihood at each iteration of the restoration process. In our application, $\gamma^{[n]}$ is estimated by a dichotomy search algorithm based on the sign of $(\mathcal{B}_{\text{DCT}} - \mathcal{B}_{\text{GGMRF}})$. We stop the procedure when the relative distance between two successive values is less than 10^{-3}. During the iterative restoration procedure, $\gamma^{[n]}$ is then refined, at each step n of the iterative restoration process, with the following procedure

$$\gamma^{[n+1]} = \begin{cases} 0.95\,\gamma^{[n]} & \text{if} \quad \mathcal{B}_{\text{GGMRF}} > \mathcal{B}_{\text{DCT}} \\ 1.05\,\gamma^{[n]} & \text{otherwise} \end{cases} \tag{9}$$

Determination of Number of Iterations: The convergence criterion of the proposed restoration procedure is empirically

Algorithm 2
GGMRF-DCT-based restoration algorithm

σ^2	Variance of the noise
T_{Hard}	Threshold value of the sparsity constraint
$\Upsilon_{T_{\text{Hard}}}$	DCT denoising (see Algo I)
$\gamma^{[n]}$	Regularization value of the GGMRF model at iteration n
$y = \hat{x}^{[0]}$	Observed (blurred and noisy) image

$$\alpha^{[n]} = \frac{\|q^{[n]}\|^2}{\|h * q^{[n]}\|^2} \quad \text{and} \quad q^{[n]} = h^{\#} * (y - h * \hat{x}^{[n]})$$

$$T_{\text{Hard}} = \begin{cases} 1.6\,\sigma & \text{if} \quad \sigma^2 < 10 \\ 2.2\,\sigma & \text{if} \quad \sigma^2 \geq 10 \end{cases}$$

I. Estimation of $\gamma^{[0]}$

$$\gamma^{[0]} = \arg\min_{\gamma^{[0]}} \left\{ \left| \left\| \Upsilon_T(\hat{x}_{\text{ML}}^{[0]}) - \hat{x}_{\text{ML}}^{[0]} \right\|_1 - \left\| \gamma^{[0]}\, \Omega'(\hat{x}^{[0]}) \right\|_1 \right| \right\}$$

with $\hat{x}_{\text{ML}}^{[0]} = \hat{x}^{[0]} + \alpha^{[0]}\, h^{\#} * (y - h * \hat{x}^{[0]})$

II. Restoration

while $n < \max\left\{400, \frac{1500}{\sigma^2}\right\}$ **do**

1. $\hat{x}_{\text{ML}}^{[n+1]} \leftarrow \hat{x}^{[n]} + \alpha^{[n]}\, h^{\#} * (y - h * \hat{x}^{[n]})$

- if n is odd

  $\hat{x}^{[n+1]} \leftarrow \hat{x}_{\text{ML}}^{[n+1]} - \gamma^{[n]}\, \Omega'(\hat{x}^{[n]})$ (see Eq. (3))

  $\triangleright\ \mathcal{B}_{\text{GGMRF}} = \left\| \gamma^{[n]}\, \Omega'(\hat{x}^{[n]}) \right\|_1$

- if n is even

  $\hat{x}^{[n+1]} \leftarrow \Upsilon_T(\hat{x}_{\text{ML}}^{[n+1]})$

  $\triangleright\ \mathcal{B}_{\text{DCT}} = \left\| \Upsilon_T(\hat{x}_{\text{ML}}^{[n+1]}) - \hat{x}_{\text{ML}}^{[n+1]} \right\|_1$

2. Iterative rescaling of $\gamma^{[n]}$ ▶

$$\gamma^{[n+1]} = \begin{cases} 0.95\,\gamma^{[n]} & \text{if} \quad \mathcal{B}_{\text{GGMRF}} > \mathcal{B}_{\text{DCT}} \\ 1.05\,\gamma^{[n]} & \text{otherwise} \end{cases}$$

$n \leftarrow n + 1$

defined by

$$\text{Number of iterations} = \max\left\{400, \frac{1500}{\sigma^2}\right\} \tag{10}$$

III. Experimental Results

A. Set Up

For the implementation of the DCT-based denoising step, we have used the fast 8×8 FFT2D DCT package implemented in C code by Takuya Ooura (functions DDCT8X8S tested in program SHRTDCT.C) and available online at http address

TABLE I
BLUR, NOISE VARIANCE AND BSNR (DB) FOR EACH EXPERIMENT

	Blur	σ^2	BSNR
Exp1	9×9 uniform [CAMERAMAN 256×256]	.308	40
Exp2	$h_{ij} = (1 + i^2 + j^2)^{-1},\ i, j = -7, \ldots, 7$ [CAMERAMAN 256×256]	2	32
Exp3	$h_{ij} = (1 + i^2 + j^2)^{-1},\ i, j = -7, \ldots, 7$ [CAMERAMAN 256×256]	8	26
Exp4	$[1, 4, 6, 4, 1]^t [1, 4, 6, 4, 1]/256$ [LENA 512×512]	49	16.5
Exp5	5×5 uniform [CAMERAMAN 256×256]	33.3	20
Exp6	$\propto [1 + (i^2 + j^2)/16]^{-3}\ \ i, j = -9, \ldots, 9$ [CAMERAMAN 256×256]	62.5	17

given in [38]. In order to compare the efficiency of our restoration model using a regularization term fusion-based procedure to a restoration model using a single GGMRF or DCT prior model, we have considered the following

1) The restoration algorithm using only the GGMRF prior model ($q = 1$). In this case, the regularization parameter γ that controls the contribution of the likelihood and prior terms is given by $\gamma = \sigma^2/6.0$, which ensures (after several trials and errors) a nearly optimal restoration result for all the experiments tested in this paper.
2) The restoration procedure using only the DCT-based complexity prior model. More precisely, this procedure simply leads to the iterative Landweber [33] procedure (Eq. (3) with $\gamma = 0$), each iterative step of which is regularized by the DCT denoising step (using the hard-thresholding rule and the estimation procedure given by Eq. (6)). For our tests, this algorithm is called the DCT gradient.
3) The proposed restoration method (summarized in pseudo code in Algorithm 2), i.e., the combined GGMRF$_{q=1}$ and DCT-based (with the hard-thresholding rule) denoising constraints with the adaptive scheme to weight the two different regularization terms and the parameter estimation procedure given by Equations (6), (8), (9) and (10).

B. Comparison with State-of-the-Art Methods

We now present a set of experimental results and comparisons illustrating the performance of the proposed approach. To this end, we have replicated the degradation models (see Table 1) generally used by several authors [1]–[7], [9]–[14], [39]–[42] [43]–[45] and we have compared the ISNR result given by our approach, i.e.,

$$\text{ISNR} = 10 \log_{10} \frac{\|x - y\|^2}{\|x - \hat{x}\|^2} \tag{11}$$

and the other published state-of-the-art methods respectively in Tables 2 and 3. In these experiments, original images are

Fig. 1. From top to bottom, original image, Noisy-blurred image for Exp1 (see Table I) and restored image using the proposed restoration approach ISNR=9.02 dB (see Table II).

Fig. 2. From top to bottom, original image, Noisy-blurred image for Exp3 (see Table I) and restored image using the proposed restoration approach ISNR=5.33 dB (see Table II).

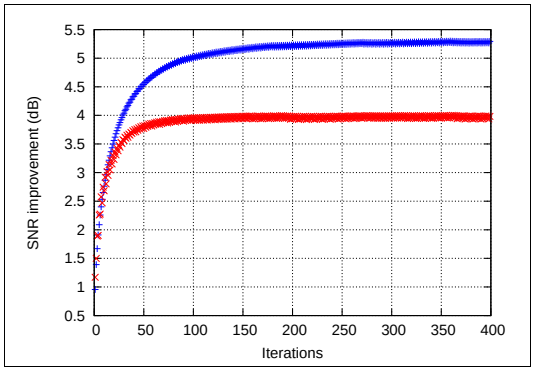

Fig. 3. Evolution of the SNR improvement for the CAMERAMAN image with the Exp3 and Exp5 degradation models.

TABLE II

PERFORMANCE COMPARISON BETWEEN OUR ALGORITHM AND OTHER RESTORATION METHODS FOR EXPERIMENTS EXP1-4

Methods	ISNR (dB) Exp1	Exp2	Exp3	Exp4
GGMRF-DCT-gradient	**9.02**	**7.76**	**5.33**	**4.48**
DCT-gradient	8.10	7.01	5.13	4.14
GGMRF-gradient	7.64	6.71	4.61	2.59
(2009) Oliveira *et al.* [7]	8.60	5.18	**7.42**	2.78
(2008) Dabov *et al.* [39]	8.34	-	-	**4.81**
(2008) Mignotte [4]	7.81	7.14	5.24	3.84
(2006) G.-Colon & Portilla [9]	7.33	7.45	5.55	-
(2006) Bioucas-Dias *et al.* [10][11]	8.52	-	-	2.97
(2006) Chantas *et al.* [1]	8.91	-	-	3.77
(2006) Foi *et al.* [2]	8.58	**8.29**	6.34	4.55
(2006) Mignotte [3]	8.23	7.58	5.70	1.63
(2006) Bioucas-Dias [13]	8.10	7.40	5.15	2.85
(2005) Figueiredo & Nowak [12]	8.16	7.46	5.24	2.84
(2004) Katkovnik *et al.* [40]	8.23	-	-	-
(2004) Neelamani *et al.* [5]	7.30	-	-	-
(2003) Figueiredo & Nowak [14]	7.59	6.93	4.88	2.94
(2001) Jalobeanu *et al.* [41]	-	6.75	4.85	-
(1998) Liu & Moulin [42]	-	-	-	1.08
(1996) Banham & Katsaggelos [6]	6.70	-	-	-

TABLE III

PERFORMANCE COMPARISON BETWEEN OUR ALGORITHM AND OTHER RESTORATION METHODS FOR EXPERIMENTS EXP5-6

Methods	ISNR (dB) Exp5	Exp6
GGMRF-DCT-gradient	**3.99**	**2.96**
DCT-gradient	3.93	2.75
GGMRF-gradient	3.35	2.47
(2008) Mignotte [4]	**4.24**	2.99
(2006) Mignotte [3]	3.50	1.90
(2000) Molina *et al.* [43]	-	2.22 (PSNR=21.1)
(1998) May *et al.* [44]	3.43	-
(1997) Charbonnier *et al.* [45] (in [43])	-	1.86 (PSNR=20.8)

TABLE IV

TIME IN SECONDS AND ITERATION NUMBER FOR EXP1-6

	Time (sec)	Iterations
Exp1	525	4869
Exp2	117	750
Exp3	62	400
Exp4	78	400
Exp5	74	400
Exp6	1068	400

CAMERAMAN (experiments 1, 2, 3, 5 and 6) of size 256×256 and LENA of size 512×512 (experiment 4). Table 1 summarizes the different degradation models used, which are defined by the blur type, the variance of the additive white Gaussian noise and the resulting BSNR

$$\text{BSNR} = 10 \log_{10} \frac{\text{VAR}(h * x)}{\sigma^2} \tag{12}$$

i.e., the ratio between the variance of the blurred image without noise and the variance of the noise for each of the experiments. The best ISNR results provided by the existing restoration algorithms and the results provided by our approach for each degradation level are indicated in bold.

C. Comparison with the SA-DCT Regularized Deconvolution

Since the SA-DCT deconvolution algorithm proposed by Foi *et al.* in [2] also uses a DCT-based denoising step, a comparison and a discussion is herein given concerning difference of models, estimation/sensitivity of the internal parameters and computational complexity of the two restoration methods. The SA-DCT regularized deconvolution algorithm proposed in [2] is a non-iterative two-step restoration procedure whose first step is essentially a deblurring stage given by a regularized Wiener filtering. The second step is a DCT filtering, applied on this resulting deblurred image, computed on several polygonal supports whose shape are defined by a preliminary segmentation technique (called LPA-ICI for local polynomial approximation - intersection of confidence intervals). To summarize, the SA-DCT in [2] thus efficiently fuses a DCT-based filtering and the result of a segmentation applied on the deblurred input image by a Wiener filtering. The segmentation used in this method (as in [3]) implicitly exploits an image prior model expressing that any real-world images can be approximated by a union of a number of nonoverlapping and distinct regions (of uniform grey level value). In comparison, our restoration algorithm aims at fusing a DCT-based sparsity and an edge preserving GGMRF-constraint which favors edge sparsity in the recovered image in order to doubly regularize an iterative deconvolution procedure. The performance of the SA-DCT regularized deconvolution algorithm depends on two regularization parameters (ϵ_1 and ϵ_2) which are manually tuned and are different for each experiment. Respectively $(0.013, 0.040)$, $(0.038, 0.045)$, $(0.062, 0.030)$ and finally $(0.10, 0.12)$ are chosen in [2] by the authors for Exp1, Exp2, Exp3 and Exp4 and are optimal for these experiments (see the Matlab procedure demo_SADCT_deblurring_copy.m available online at http address given in [2]). By comparison, our restoration method relies on one regularization function (see Eq. (6)) which is the same for all images and degradation models.

D. Discussion

Table 6 shows the time in seconds and the number of iterations that each restoration took for each one of the considered degradation models according to Eq. (10) (cf. Table 1) and for our algorithm (cf. Algorithm 2) (system used: AMD Athlon 64 Processor 3500+, 2.2 GHz, 4435.67 bogomips and non-optimized code running on Linux). The source code (in C++

language) for our algorithm (with the set of initial, degraded and restored images) is publicly available at the following http address www.iro.umontreal.ca/∼mignotte/ResearchMaterial/ in order to make possible eventual comparisons with future restoration methods. Note that our restoration procedure could be computationally optimized since numerous fast Very Large Scale Integration (VLSI) chips exist for computing the DCT transform more quickly.

We can notice that the proposed method leads to competitive restoration results for various levels of blur and noise degradations in benchmark tests and provides a good compromise between restoration results for the high and low BSNR case. In addition, the proposed restoration method, combining the GGMRF and DCT constraints always significantly improves the ISNR result compared to a single GGMRF or DCT prior model in all the considered degradation models. This tends to demonstrate the ability of our strategy to efficiently fuse these two different constraints on the restoration result. Figures 1 and 2 show visually some restoration results for Exp1 and Exp3[2]. Let us also add that the estimation of T_{Hard} (which then ensures the estimation of γ) and the number of iterations could be improved since better ISNR results can be achieved if we supervise (by manually tuning) these two values for each tested experimental result presented in this paper. Fig. 3 shows the evolution of the ISNR and its convergence as a function of the number of iterations for respectively the degradation models Exp3 and Exp4. The soft-thresholding rule (Algorithm 1, step 2) does not improve the ISNR results compared to the hard-thresholding rule used in our GGMRF-DCT-based restoration procedure. The ISNR results for the different experiments are equivalent or not as good. More precisely, we respectively obtain for the different experiments; Exp1 : 7.35 dB Exp2 : 7.25 dB Exp3 : 5.08 dB Exp4 : 3.88 dB Exp5 : 3.51 dB Exp6 : 2.91 dB. Visually and compared to [2], the restoration results are similar for noisy images with low BSNR (i.e., degradations exhibiting more noise than blur) and our restoration method provides visually better restored images for high BSNR (i.e., degradations exhibiting more blur than noise), which is also confirmed by a higher improvement SNR measure.

It is also worth recalling that, contrary to [2], [15]–[21], our strategy is especially suited to fuse (or combine) several other (and not only two) regularizers or penalty terms. In addition, in our method, these penalty terms or regularizers can be very different in nature (e.g., hard constraints, energy penalty terms, thresholding in the frequential domain, projection onto convex sets (POCS), filtering, etc.). To give an example, our fusion model would easily allow to combine a POCS method as first regularizer in conjunction with a second wavelet-based prior/regularizer (using, for example, a shrinkage-thresholding function). In this context, our constraint A1 would allow to iteratively adapt $\gamma^{[n]}$ (see Algorithm 2) in order that for each iteration of the Landweber (deblurring) algorithm, giving the likelihood image $\hat{x}_{\text{ML}}$, the residual image added to $\hat{x}_{\text{ML}}$ by the POCS constraint and the residual image added to $\hat{x}_{\text{ML}}$ by the shrinkage-thresholding operation in the wavelet domain should be equal in a norm sense.

[2]Additional examples (i.e., degraded and restored image results) are also given in http: www.iro.umontreal.ca/∼mignotte/ResearchMaterial/

IV. Conclusion

In this paper, we have presented an efficient and simple doubly regularized restoration procedure combining efficiently two different regularization strategies respectively expressed in the spatial and frequency domains. Due to an adaptive and rescaling scheme, used to balance the influence of these two different regularizers, the resulting restoration strategy performs competitively among the recently reported state-of-the-art restoration schemes for different BSNR, blur and noise levels, while being simple to implement. This fusion of regularization terms can be a simple way to better model the intrinsic and complex properties of the original undegraded image to be recovered by simultaneously incorporating different types of knowledge concerning the types of restorations *a priori* defined as acceptable solutions.

Acknowledgment

The author would like to thank the anonymous reviewers for their many valuable comments and suggestions that helped to improve both the technical content and the presentation quality of this paper.

References

[1] G. Chantas, N. Galatsanos, and A. Likas, "Bayesian restoration using a new nonstationary edge-preserving image prior," *IEEE Trans. Image Processing*, vol. 15, no. 10, pp. 2987–2997, 2006.

[2] A. Foi, K. Dabov, V. Katkovnik, and K. Egiazarian, "Shape-adaptive DCT for denoising and image reconstruction," in *Proceeding of SPIE Electronic Imaging 2006, Image Processing: Algorithms and Systems V*, vol. 6064A-18, http://www.cs.tut.fi/∼foi/SA-DCT/, January 2006.

[3] M. Mignotte, "A segmentation-based regularization term for image deconvolution," *IEEE Trans. Image Processing*, vol. 15, no. 7, pp. 1973–1984, 2006.

[4] ——, "A non-local regularization strategy for image deconvolution," *Pattern Recognition Letters*, vol. 29, no. 16, pp. 2206–221, December 2008.

[5] R. Neelamani, H. Choi, and R. Baraniuk, "ForWaRD: Fourier-wavelet regularized deconvolution for ill-conditioned systems," *IEEE Trans. Signal Processing*, vol. 52, no. 2, pp. 418–433, 2004.

[6] M. R. Banham and A. K. Katsaggelos, "Spatially adaptive wavelet-based multiscale image restoration," *IEEE Trans. Image Processing*, vol. 5, no. 4, pp. 619–634, 1996.

[7] J. Oliveira, J. Bioucas-Dias, and M. Figueiredo, "Adaptive total variation image deblurring: A majorization-minimization approach," *Signal Processing*, vol. 89, no. 9, pp. 1683–1693, September 2009.

[8] L. Rudin, S. Osher, and E. Fatemi, "Nonlinear total variation based noise removal algorithms," *Phys. D*, vol. 60, pp. 259–268, 1992.

[9] J. A. Guerrero-Colon and J. Portilla, "Deblurring-by-denoising using spatially adaptive gaussian scale mixtures in overcomplete pyramids," in *IEEE International Conference on Image Processing (ICIP'06)*, vol. I, Atlanta, GA, USA, October 2006, pp. 625–628.

[10] J. Bioucas-Dias, M. Figueiredo, and J. Oliveira, "Adaptive total-variation image deconvolution: A majorization-minimization approach," in *Proceeding of EUSIPCO'2006*, Florence, Italy, September 2006.

[11] ——, "Total variation image deconvolution: A majorization-minimization approach," in *IEEE International Conference on Acoustics, Speech, and Signal Processing (ICASSP'2006)*, vol. II, Toulouse, French, May 2006.

[12] M. Figueiredo and R. Nowak, "A bound optimization approach to wavelet-based image deconvolution," in *IEEE International Conference on Image Processing (ICIP'05)*, vol. II, Genova, Italy, September 2005, pp. 782–785.

[13] J. Bioucas-Dias, "Bayesian wavelet-based image deconvolution: a GEM algorithm exploiting a class of heavy-tailed priors," *IEEE Trans. Image Processing*, vol. 15, no. 4, pp. 937–951, 2006.

[14] M. A. T. Figueiredo and R. D. Nowak, "An EM algorithm for wavelet-based image restoration," *IEEE Trans. Image Processing*, vol. 12, no. 8, pp. 906–916, 2003.

[15] F. Malgouyres, "Minimizing the total variation under a general convex constraint for image restoration," *IEEE Trans. Image Processing*, vol. 11, no. 12, pp. 1450–1456, Dec. 2001.

[16] E. J. Candes and F. Guo, "New multiscale transforms, minimum total variation synthesis: applications to edge-preserving image reconstruction," *Signal Processing*, vol. 82, no. 11, pp. 1519–1543, Nov. 2002.

[17] S. Durand and J. Froment, "Reconstruction of wavelet coefficients using total variation minimization," *SIAM Journal on Scientific Computing*, vol. 24, no. 5, pp. 1754–1767, 2002.

[18] H. Z. T. Chan, "Total variation improved wavelet thresholding in image compression," in *IEEE International Conference on Image Processing (ICIP'00)*, Vancouver, BC, CA, Sept. 2000, pp. 1289–1302.

[19] D. Zhu, M. Razaz, and M. Fisher, "An adaptive algorithm for image restoration using combined penalty functions," *Pattern Recognition Letters*, vol. 27, no. 12, pp. 1336–1341, Sept. 2006.

[20] M. Lysaker and X.-C. Tai, "Iterative image restoration combining total variation minimization and a second-order functional," *International Journal of Computer Vision*, vol. 66, no. 1, pp. 5–18, Jan. 2006.

[21] F. Li, C. Shen, J. Fan, and C. Shen, "Image restoration combining a total variational filter and a fourth-order filter," *Journal of Visual Communication and Image Representation*, vol. 18, no. 4, pp. 322–330, Aug. 2007.

[22] G. Chantas, N. P. Galatsanos, and A. Likas, "Bayesian image restoration based on variational inference and a product of student-t priors," in *Proceedings of the IEEE International MLSP Workshop*, Thessaloniki, Greece, August 2007.

[23] G. Chantas, N. Galatsanos, A. Likas, and M. Saunders, "Variational bayesian image restoration based on a product of t-distributions image prior," *IEEE Trans. Image Processing*, vol. 17, no. 10, pp. 1795–1805, 2008.

[24] G. Chantas, N. Galatsanos, R. Molina, and A. K. Katsaggelos, "Variational bayesian image restoration with a product of spatially weighted total variation image priors," *IEEE Trans. Image Processing*, vol. 19, no. 2, pp. 351–356, 2010.

[25] K. Dabov, A. Foi, V. Katkovnik, and K. Egiazarian, "Image denoising by sparse 3-d transform-domain collaborative filtering," *IEEE Trans. Image Processing*, vol. 16, no. 8, pp. 2080 – 2095, 2007.

[26] A. Foi, V. Katkovnik, and K. Egiazarian, "Pointwise shape-adaptive dct for high-quality denoising and deblocking of grayscale and color images," *IEEE Trans. Image Processing*, vol. 16, no. 5, pp. 1395 – 1411, 2007.

[27] M. Mignotte, J. Meunier, and J.-P. Soucy, "Dct-based complexity regularization for em tomographic reconstruction," *IEEE Trans. Biomed. Eng.*, vol. 55, no. 2, pp. 801–805, 2008.

[28] C. A. Bouman and K. Sauer, "A unified approach to statistical tomography using coordinate descent optimization," *IEEE Trans. Image Processing*, vol. 5, no. 3, pp. 480–492, 1996.

[29] S. Haykin, *Neural Networks: A comprehensive Foundation*. Prenctice Hall, Inc., 1999.

[30] T. Dietterich, "Ensemble methods in machine learning," in *Proceedings of the First International Workshop on Multiple Classifier Systems, LNCS, Multiple Classifier Systems*, L. N. I. C. Science, Ed., vol. 1857. Springer, 2000, pp. 1–15.

[31] C. A. Bouman and K. Sauer, "A generalized Gaussian image model for edge-preserving MAP estimation," *IEEE Trans. Image Processing*, vol. 2, no. 3, pp. 296–310, 1993.

[32] B. J. Sullivan and H.-C. Chang, "A generalized landweber iteration for ill-conditioned signal restoration," in *IEEE International Conference on Acoustics, Speech, and Signal Processing (ICASSP'91)*, Toronto, Ontario, Canada, April 1991, pp. 1729–1732.

[33] L. Landweber, "An iterative formula for fredholm integral equations of the first kind," *American Journal of Mathematics*, vol. 73, pp. 615–624, 1951.

[34] E. Simoncelli, "Bayesian denoising of visual image in the wavelet domain," *Bayesian Inference in Wavelet Based Models. eds. P. Mller and B. Vidakovic. Springer-Verlag, Lecture Notes in Statistics 141*, March 1999.

[35] D. L. Donoho and I. M. Johnstone, "Ideal spatial adaptation by wavelet shrinkage," *Biometrika*, vol. 81, pp. 425–455, December 1994.

[36] H. S. Malavar, *Signal Processing with Lapped Transforms*. Norwood, MA, Artech House, 1992.

[37] R. Coifman and D. Donohu, "Translation invariant denoising," in *Wavelets and Statistics, Lecture Notes in Statistics*, vol. 103. A. Antoniadis and G. Oppenheim, Eds. New York:Springer-Verlag, 1995, pp. 125–150.

[38] T. Ooura, "General purpose FFT (fast fourier/cosine/sine transform) package," http://momonga.t.u-tokyo.ac.jp/∼ooura/fft.html.

[39] K. Dabov, A. Foi, V. Katkovnik, and K. Egiazarian, "Image restoration by sparse 3d transform-domain collaborative filtering," in *Proceedings of SPIE, the International Society for Optical Engineering Image Processing: Algorithms and Systems VI*, vol. 6812-07, San Jose, CA, USA, January 2008.

[40] V. Katkovnik, A. Foi, K. Egiazarian, and J. Astola, "Directional varying scale approximations for anisotropic signal processing," in *Proceedings of XII European Signal Processing Conference, EUSIPCO 2004,*, Vienna, Austria, 2004, pp. 101–104.

[41] A. Jalobeaunu, N. Kingsbury, and J. Zerubia, "Image deconvolution using hidden Markov tree modeling of complex wavelet packets," in *IEEE International Conference on Image Processing (ICIP'01)*, vol. I, Thessaloniki, Greece, October 2001, pp. 201–204.

[42] J. Liu and P. Moulin, "Complexity-regularized image restoration," in *IEEE International Conference on Image Processing (ICIP'98)*, vol. I, Chicago, Illinois, USA, October 1998, pp. 555–559.

[43] R. Molina, A. K. Katsaggelos, J. Mateos, A. Hermoso, and C. A. Segall, "Restoration of severely blurred high range images using stochastic and deterministic relaxation algorithms in compound Gauss-Markov random fields," *Pattern Recognition*, vol. 33, no. 4, pp. 555–571, 2000.

[44] K. May, T. Stathaki, A. G. Constantinides, and A. K. Katsaggelos, "Iterative determination of local bound constraints in iterative image restoration," in *IEEE International Conference on Image Processing (ICIP'98)*, vol. II, Chicago, Illinois, USA, October 1998, pp. 833–836.

[45] P. Charbonnier, L. Blanc-Feraud, G. Aubert, and M. Barlaud, "Deterministic edge-preserving regularization in computed imaging," *IEEE Trans. Image Processing*, vol. 5, no. 12, pp. 298–311, 1997.

Max Mignotte received the DEA (Postgraduate degree) in Digital Signal, Image and Speech processing from the INPG University, France (Grenoble), in 1993 and the Ph.D. degree in electronics and computer engineering from the University of Bretagne Occidentale (UBO) and the digital signal laboratory (GTS) of the French Naval academy, France, in 1998. He was an INRIA post-doctoral fellow at University of Montreal (DIRO), Canada (Quebec), from 1998 to 1999. He is currently with DIRO at the Computer Vision & Geometric Modeling Lab as an associate Professor (Professeur agrégé) at the University of Montreal. He is also a member of LIO (Laboratoire de recherche en imagerie et orthopedie, Centre de recherche du CHUM, Hopital Notre-Dame) and researcher at CHUM. His current research interests include statistical methods, Bayesian inference and hierarchical models for high-dimensional inverse problems such as segmentation, parameters estimation, fusion, shape recognition, deconvolution, 3D reconstruction and restoration problems.